

Carbon Nanotube Growth from Semiconductor Nanoparticles

Daisuke Takagi,[†] Hiroki Hibino,[‡] Satoru Suzuki,[‡] Yoshihiro Kobayashi,^{‡,§} and Yoshikazu Homma^{*,†,§}

*Department of Physics, Tokyo University of Science, Shinjuku, Tokyo 162-8601, Japan,
NTT Basic Research Laboratories, NTT Corporation, Atsugi,
Kanagawa 243-0198, Japan, and CREST, Japan Science and Technology Agency,
Chiyoda, Tokyo 102-0075, Japan*

Received April 4, 2007; Revised Manuscript Received June 20, 2007

ABSTRACT

Nanoscale metal catalysts have been indispensable for carbon nanotube (CNT) synthesis by chemical vapor deposition (CVD). We show that even semiconductor nanoparticles of SiC, Ge, and Si produce single-walled and double-walled CNTs in CVD with ethanol. This implies that nanosize structures might act as a template for the formation of CNT caps composed of five- and six-membered rings. Providing a template for cap formation is the essential role of the catalysts.

Controlled synthesis of carbon nanotubes (CNTs) is a major issue for their applications to nanoscale electronics and photonics. Nanoscale metal catalysts have been indispensable for CNT synthesis by chemical vapor deposition (CVD), which is commonly used for CNT synthesis on substrates.¹ Metal catalysts are thought to work by (i) decomposing hydrocarbon molecules, (ii) precipitating carbon atoms on the catalyst particle surface, and (iii) forming a graphite cylinder. Effective catalysts have been limited to iron, cobalt, nickel, and palladium, which have a catalytic function to produce graphite on bulk crystal surface.² Recently, however, gold, silver, and copper have been reported to produce CNTs.^{3–5} This implies that hydrocarbon-molecule decomposition and graphite formation abilities are not essential and leads to a new interpretation of the role of catalyst particle in CNT growth: only a nanoscale curvature would be necessary to grow CNTs if carbon atoms are supplied to the nanocurvature.

Here, we report experimental evidence supporting the above hypotheses: CNT formation on semiconductor nanoparticles of SiC, Ge, and Si, with which no catalytic functions were expected, in CVD with ethanol. Grown CNTs are single-walled (SWCNTs) or double-walled (DWCNTs), with a diameter of 5 nm or smaller.

SiC nanoparticles were formed on Si(111) substrate. To clean the Si substrate, we used H₂SO₄/H₂O₂ (4:1) oxidation (for 5 min) followed by buffered-HF etching (for 1 min). Finally, the Si substrate was soaked in C₂H₅OH solution for

3 min. After wet treatments, SiC crystalline nanoparticles with the epitaxial relationship of (111)/(111) were formed by heating the Si(111) substrate at around 1000 °C in an ultrahigh vacuum (UHV). The source of carbon was carbon-bearing molecules desorbed from the sample or the sample holder. Ge and Si nanoparticles were formed on 6H-SiC(0001) substrates. To clean the SiC substrate, we used H₂SO₄/H₂O₂ (4:1) oxidation (for 5 min) followed by buffered-HF etching (for 1 min). After final oxidation in H₂SO₄/H₂O₂ (4:1) (for 5 min), annealing and Si deposition on the SiC substrate were done at around 1000 °C in UHV. By annealing and Si deposition, the surface structure of SiC changed from 1 × 1 (before annealing), to $\sqrt{3} \times \sqrt{3}$ (after 1000 °C annealing), and finally to 3 × 3 (after Si deposition). Ge or Si was deposited on the 6H-SiC(0001)3 × 3 surface at room temperature. For Ge and Si, crystalline nanoparticles with the epitaxial relationships of both (111)/(0001) and (110)/(0001) were formed by annealing the substrate at 400 °C.^{6,7}

For CNT synthesis, high-temperature air heating and ethanol CVD were performed successively, the same as the case of gold, silver, and copper.³ First, the substrate was introduced into the furnace, which had been preheated to 900 °C. The introduction and heating were done in air at atmospheric pressure. The duration of air heating was 1–10 min depending on the particle species and size. Then, air was evacuated with a rotary pump down to 1×10^2 Pa and replaced by Ar/H₂ (3% H₂ by volume) with the pressure of 9×10^4 Pa. To remove the oxide formed on the catalyst particles during air heating, the sample was kept in the 900 °C Ar/H₂ ambience for 10 min. Then the temperature was set to 850 °C, and the CVD growth was performed by

* Corresponding author. E-mail: homma@rs.kagu.tus.ac.jp.

[†] Department of Physics, Tokyo University of Science.

[‡] NTT Basic Research Laboratories.

[§] CREST, Japan Science and Technology Agency.

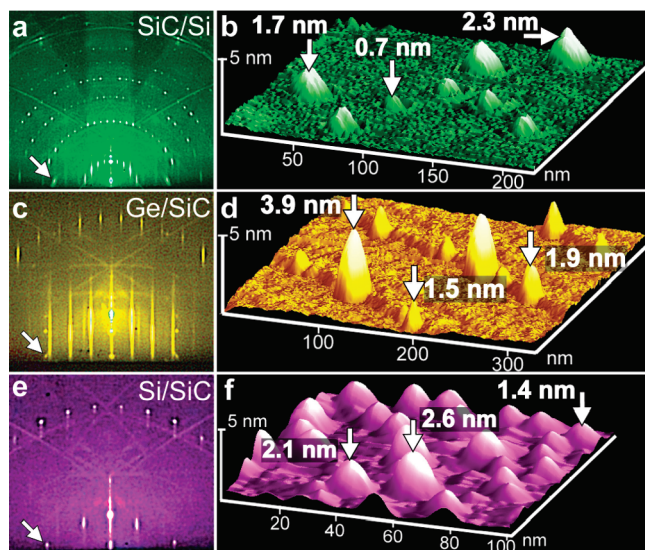


Figure 1. RHEED patterns and AFM images of epitaxially grown semiconductor nanoparticles. (a) RHEED pattern of epitaxially grown SiC nanoparticles on Si(111)7×7. A 20 kV electron beam was incident from the [112] azimuth. The arrow indicates a transmission diffraction spot of SiC(111) plane. (b) AFM image of SiC nanoparticles. Size distribution is 1.2 ± 0.5 nm. (c) RHEED pattern of epitaxially grown Ge nanoparticles on SiC(0001). The arrow indicates a transmission diffraction spot of Ge(111) plane. (d) AFM image of Ge nanoparticles. Size distribution is 1.7 ± 1.4 nm. (e) RHEED pattern of epitaxially grown Si nanoparticles on SiC(0001). The arrow indicates a transmission diffraction spot of Si(111) plane. (f) AFM image of Si nanoparticles. Size distribution is 1.3 ± 0.7 nm.

bubbling liquid ethanol using Ar/H₂ gas for 10–30 min at $5\text{--}7 \times 10^2$ Pa. The flow rate of the bubbling gas was about 50 sccm (standard cubic centimeter per minute).

To synthesize CNTs using semiconductor nanoparticles, it is essential to use particles 5 nm or smaller. We prepared such particles in UHV while observing reflection high-energy electron diffraction (RHEED). SiC nanoparticles were formed on Si(111) substrate, and Ge and Si nanoparticles were formed on SiC(0001) substrates. Figure 1a is a RHEED pattern from SiC nanoparticles on Si substrate. The transmission diffraction spots, one of which is denoted by an arrow, indicate that SiC crystalline particles have epitaxial relationship with the Si(111) substrate.⁸ The atomic force microscope (AFM) image of the surface in Figure 1b shows that the nanoparticle size is less than 5 nm. Similarly, Ge and Si crystalline nanoparticles were formed on SiC(0001) substrates. RHEED patterns and AFM images of those particles are shown in Figures 1c–f. The RHEED patterns confirm the epitaxial relationships of Ge(111)/SiC(0001) and Si(111)/SiC(0001), and the AFM images reveal that Ge and Si nanoparticle sizes are less than 5 nm.

CNTs were grown using those nanoparticles by supplying carbon atoms thermally decomposed from ethanol at 850 °C. Heating in air is the key technique for CNT synthesis from semiconductor nanoparticles. Prior to supplying ethanol, we cleaned the sample by 900 °C heating in air. This process removes carbon contaminants on the nanoparticles.³ It should also cause oxidation of nanoparticles, but the core of the semiconductor nanoparticles remained unoxidized as dis-

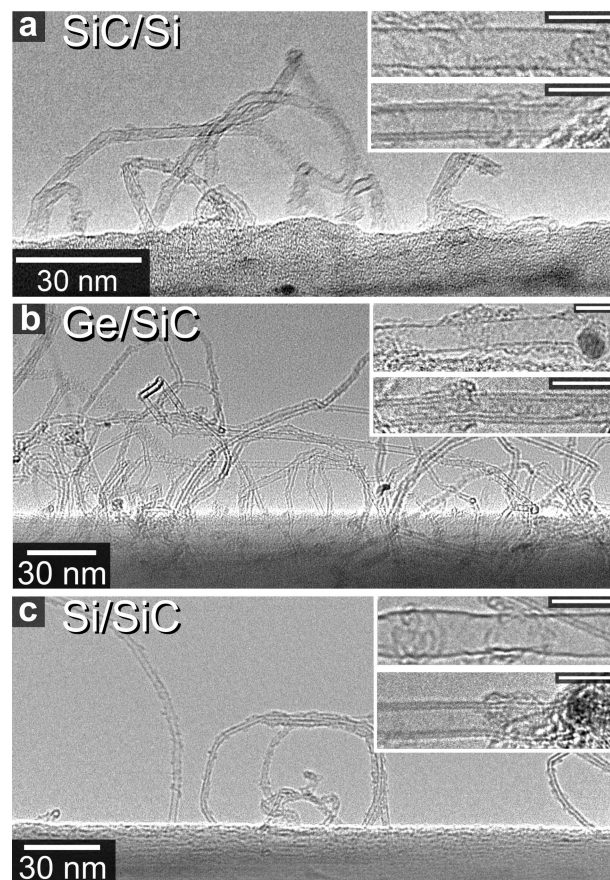


Figure 2. TEM images of CNTs grown from semiconductor nanoparticles of (a) SiC, (b) Ge, and (c) Si. Upper and lower insets are high-resolution images of SWCNTs and DWCNTs, respectively. Inset scale bars: 5 nm.

cussed later. The surface oxide layer should be reduced or sublimated by succeeding heating in Ar/H₂, and resulting clean particles should contribute to CNT growth.

Transmission electron microscope (TEM) images are shown in Figure 2 for CNTs grown from SiC, Ge, and Si nanoparticles. In all cases, CNT growth was confirmed. They are not very straight and forming looped shapes. High-resolution images in the insets show that these CNTs are either single-walled or double-walled. For Ge and Si nanoparticles, the root part including a catalyst particle could be observed. However, lattice fringes of the particles could not be observed because it was difficult to adjust the electron beam incidence to the crystalline orientation of the particular nanoparticles. The CNT yield from Ge nanoparticles is higher than those from SiC and Si nanoparticles. The melting point of Ge is much lower than those of SiC and Si. It is plausible that Ge nanoparticles are molten during CVD, which might be related to the higher CNT yield.

Raman scattering spectra from grown CNTs are shown in Figure 3. Signals due to the radial-breathing mode (RBM) were detected in all cases.⁹ Two excitation-laser wavelengths were used to probe a wide range of CNT chiralities. Metallic CNTs with diameters of 1.2–1.3 nm produce RBM at around 185–210 cm⁻¹ with 633 nm excitation-laser wavelength, and semiconducting CNTs with diameters of 1.3–1.5 nm produce RBM at around 165–190 cm⁻¹ with 532 nm excitation-laser

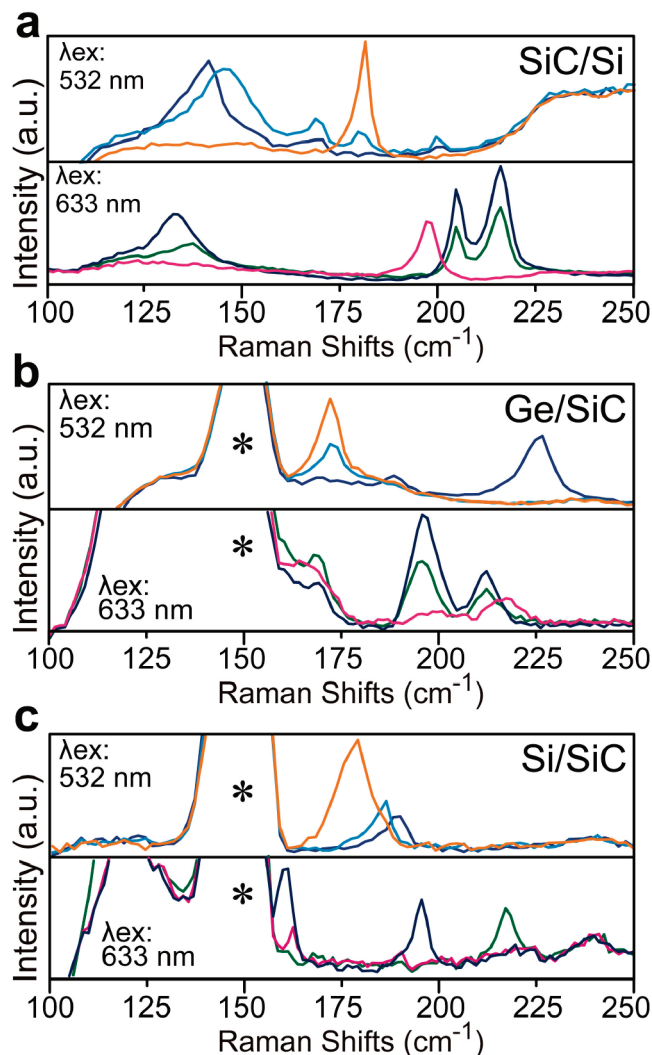


Figure 3. Raman spectra of CNTs grown from semiconductor nanoparticles of (a) SiC, (b) Ge, and (c) Si. The upper and lower spectra were obtained using excitation-laser wavelengths (λ_{ex}) of 532 and 633 nm, respectively. Spectra from three measurement points are overlain in each panel. The signals indicated by an asterisk originate from the SiC substrate.

wavelength.¹⁰ For all the nanoparticle species, RBM peaks originated from both metallic and semiconducting CNTs are seen. Large signals indicated by asterisks originate from the SiC substrate.¹¹

The CNT diameters observed in the TEM images in Figure 2 are 3–4 nm and are larger than those derived from RBM peaks. Such large-diameter CNTs produce RBM peaks at less than 100 cm^{-1} , which could not be detected with the present Raman spectrometer. In TEM, CNTs lifting off the substrate were selectively observed. Those lifting CNTs are curled or looped, showing that they are defective. On the other hand, straight CNTs tend to lie on the surface when they grow longer than about 100 nm.¹² Large-diameter and defective CNTs did not fall on the substrate surface and thus could be observed by TEM.

We did not see any clear differences in the CNT diameter distributions among SiC, Ge, and Si catalysts. There seems to be no preference of chirality for each catalyst species. Even if there were any catalyst–species dependences, a broad

size distribution of nanoparticles made it difficult to elucidate the catalyst–species dependences.

The present study demonstrates that SWCNTs and DWCNTs are produced from SiC, Ge, and Si nanoparticles. The chemical state and phase of the nanoparticles during CVD are of great interest. Although they were exposed to high-temperature air before the CVD process, the core of nanoparticle was expected to remain unoxidized. This is because compressive stress induced by surface oxidation prevents full oxidation of the nanoparticles.¹³ The thin oxide layer formed in the air heating can easily be sublimated at the CVD temperature.^{14,15} However, we do not exclude the possibility of contribution of oxide on CNT growth at present.

Concerning the phase of the catalyst particles in the CVD ambience, Ge nanoparticles can be molten at 850 °C because the melting point of bulk Ge is 937 °C and melting point reduction is expected for nanoparticles.¹⁶ On the other hand, SiC nanoparticles might remain solid during CVD, because SiC particles on a Si surface only sublime without melting. In UHV, we have confirmed that the SiC nanoparticles used for CNT growth were single crystalline even at 1000 °C by RHEED (Figure S1, Supporting Information). For Si nanoparticles, although we have no experimental evidence, we think that Si nanoparticles were solid during CVD because of the high bulk melting point, 1410 °C, and the strong covalent bond. The covalent Si and SiC cases are different from metal particles whose thermal stability is governed by weak metallic bonds.

Unlike the conventional metal catalysts, iron, cobalt, and nickel, for CNT synthesis, semiconductors as well as gold, silver, and copper, in their bulk form, do not have a catalytic function to produce graphite. And even those materials, when they become nanosize particles, can form CNTs. This implies that carbon atoms on a nanoparticle can assemble themselves into CNTs. Nanosize structures with a curvature of 5 nm or smaller might act as a template for the formation of CNT caps composed of five- and six-membered rings. Providing a template should be the essential role of the catalysts. Then, we speculate the CNT growth mechanism as follows. Nanoparticles can be liquid^{17,18} or solid¹⁹ in the CVD ambience. Most metal nanoparticles and Ge are molten during CVD, while SiC and Si particles might remain solid. When the catalyst is liquid, carbon atoms are soluble in it. In the solid case, carbon atoms are adsorbed on the surface of the catalyst. Or, catalyst and carbon atoms may form a noncrystalline cluster.²⁰ In any case, carbon atoms precipitated or adsorbed on the nanoparticle surface may assemble themselves to form CNT caps. Once a cap is created, it acts as a nucleus and carbon atoms on the nanoparticle are incorporated into the edge of the cap, forming a graphite sheet cylinder as a nanotube (root growth mechanism).²¹ On a flat surface, on the other hand, even if a graphite sheet is formed, its surface is inert and graphite growth is terminated at one monolayer. For liquid phase, our interpretation would be within the framework of the vapor–liquid–solid (VLS) mechanism of nanotube growth.^{17,21} However, the VLS mechanism only explains selective carbon uptake into

nanodroplets and supersaturation of carbon, and it does not tell how a cap is created. A theoretical support of cap creation on a curved surface could be found in ref 22, although it was only successful on the iron particle surface.

We should comment on the yield of CNTs from the new catalyst species. Although we could not get quantitative data, the yield was much lower for SiC, Ge, and Si than for iron group metals iron, cobalt, and nickel. As mentioned above, Ge nanoparticles had a higher CNT yield compared to SiC and Si nanoparticles. The CNT yield of gold, silver, and copper lay in the intermediate of iron group metals and semiconductors. The difference in the CNT yield might reflect the catalytic activity of ethanol decomposition. SiC, Ge, and Si should have little activity of ethanol decomposition. Thus, a higher growth temperature, 850 °C, was essential to induce pyrolysis of ethanol. The phase of the nanoparticle, solid or liquid, would also affect the CNT yield, because it relates to the precipitation mechanism of carbon atoms on the nanoparticle surface.

The self-assembling nature of CNTs on a nanoparticle has important meaning in the growth control and application of CNTs. "Catalyst-free" synthesis of CNTs would be possible by using nanoscale roughness with a high density. The nanoscale structures can have a single-crystalline orientation, as suggested for SiC particles. By selecting a suitable material or a crystal structure, chirality-controlled CNT growth would be possible from nanocrystals in a single-crystalline orientation.

Acknowledgment. We thank Hiroko Takahata and Seichiro Mizuno, NTT Advanced Technology Corporation, for TEM observations.

Supporting Information Available: Reflection high-energy electron diffraction pattern of epitaxially grown SiC nanoparticles on Si(111) observed at 850 and 1000 °C in ultrahigh vacuum. This material is available free of charge via the Internet at <http://pubs.acs.org>.

References

- (1) Kong, J.; Cassell, A. M.; Dai, H. *Chem. Phys. Lett.* **1998**, 292, 567–574.
- (2) Hamilton, J. C.; Blakely, J. M. *Surf. Sci.* **1980**, 91, 199–217.
- (3) Takagi, D.; Homma, Y.; Hibino, H.; Suzuki, S.; Kobayashi, Y. *Nano Lett.* **2006**, 6, 2642–2645.
- (4) Bhaviripudi, S.; Mile, E.; Steiner, S. A.; Zare, A. T.; Dresselhaus, M. S.; Belcher, A. M.; Kong, J. *J. Am. Chem. Soc.* **2007**, 129, 1516–1517.
- (5) Zhou, W. W.; Han, Z. Y.; Wang, J. Y.; Zhang, Y.; Jin, Z.; Sun, X.; Zhang, Y. W.; Yan, C. H.; Li, Y. *Nano Lett.* **2006**, 6, 2987–2990.
- (6) Aït-Mansour, K.; Kubler, L.; Dentel, D.; Bischoff, J. L.; Diani, M.; Feuillet, G. *Surf. Sci.* **2003**, 546, 1–11.
- (7) Fissel, A.; Akhtariev, R.; Richter, W. *Thin Solid Films* **2000**, 380, 42–45.
- (8) Ino, S. *Jpn. J. Appl. Phys.* **1977**, 16, 891–908.
- (9) Rao, A. M.; Richter, E.; Bandow, S.; Chase, B.; Eklund, P. C.; Williams, K. A.; Fang, S.; Subbaswamy, K. R.; Menon, M.; Thess, A.; Smalley, R. E.; Dresselhaus, G.; Dresselhaus, M. S. *Science* **1997**, 275, 187–191.
- (10) Kataura, H.; Kumazawa, Y.; Maniwa, Y.; Umez, I.; Suzuki, S.; Ohtsuka, Y.; Achiba, Y. *Synth. Met.* **1999**, 103, 2555–2558.
- (11) Murakami, T.; Sako, T.; Harima, H.; Kisoda, K.; Mitikami, K.; Ishiki, T. *Thin Solid Films* **2004**, 464–65, 319–322.
- (12) Takagi, D.; Homma, Y.; Suzuki, S.; Kobayashi, Y. *Surf. Interface Anal.* **2006**, 38, 1743–1746.
- (13) Kohno, H.; Takeda, S. *Appl. Phys. Lett.* **1998**, 73, 3144–3146.
- (14) Surnev, L.; Tikhov, M. *Surf. Sci.* **1982**, 123, 505–518.
- (15) Kobayashi, Y.; Shinoda, Y.; Sugii, K. *Jpn. J. Appl. Phys.* **1990**, 29, 1004–1008.
- (16) Moisala, A.; Nasibulin, A. G.; Kauppinen, E. I. *J. Phys.: Condens. Matter* **2003**, 15, S3011–S3035.
- (17) Homma, Y.; Kobayashi, Y.; Ogino, T.; Takagi, D.; Ito, R.; Jung, Y. J.; Ajayan, P. M. *J. Phys. Chem. B* **2003**, 107, 12161–12164.
- (18) Harutyunyan, A. R.; Tokune, T.; Mora, E. *Appl. Phys. Lett.* **2005**, 87, 051919-1–051919-3.
- (19) Hofmann, S.; Sharma, R.; Ducati, C.; Du, G.; Mattevi, C.; Cepek, C.; Cantoro, M.; Pisana, S.; Parvez, A.; Cervantes-Sodi, F.; Ferrari, A. C.; Dunin-Borkowski, R.; Lizzit, S.; Petaccia, L.; Goldoni, A.; Robertson, J. *Nano Lett.* **2007**, 7, 602–608.
- (20) Shibuta, Y.; Maruyama, S. *Chem. Phys. Lett.* **2003**, 382, 381–386.
- (21) Gavillet, J.; Loiseau, A.; Journet, C.; Willaime, F.; Ducastelle, F.; Charlier, J.-C. *Phys. Rev. Lett.* **2001**, 87, 275504-1–275504-4.
- (22) Raty, J.-Y.; Gygi, F.; Galli, G. *Phys. Rev. Lett.* **2005**, 95, 096103-1–096103-4.

NL0708011